

GRANULOMETRIC LIMITS OF HYPOPLASTIC MODELS

IWO HERLE

*Institute of Theoretical and Applied Mechanics,
Czech Academy of Sciences,
Prosecká 76, 190 00 Praha 9, Czech Republic
herle@itam.cas.cz*

(Received 29 May 2000)

Abstract: Several successful applications of the hypoplastic models would not be possible without a reliable and simple calibration procedure of the model parameters. The procedure utilizing standard properties of grain assemblies is well-suited for sands and is briefly outlined here. However, there are limits for the application of this approach for other soils. This is demonstrated for a coarse-grained limestone rockfill and a fined-grained loess. Whereas the parameter determination of the limestone rockfill is mainly limited by the available laboratory equipment, the calibration procedure must be significantly modified for the loess soil. Finally, a serious problem concerning the application of the hypoplastic model for soils with low friction angles is discussed. It is shown that in this case the ratio of incremental stiffness moduli in triaxial and isotropic compression is unrealistically low.

Keywords: hypoplastic law, calibration, constitutive parameters, sand, limestone rockfill, clay, loess soil

1. Introduction

Hypoplastic constitutive models [16, 18, 30, 7, 27, 20] based on the proposal of Kolymbas [15] have proven to be very successful in reproducing the mechanical behaviour of granular soils¹. Their recent formulations can realistically capture the influence of mean pressure and density along various deformation paths and the soil behaviour is bounded by asymptotic states [8, 2] including the widely accepted critical states [24]. Without the decomposition of strains into elastic and plastic parts, the mathematical structure of hypoplastic equations remains simple. A single

¹This group of constitutive models was mainly developed at the University of Karlsruhe, Germany, whereas a parallel development of slightly different hypoplastic models was performed in Grenoble, France [3].

tensorial equation for the evolution of effective stress does not encompass any yield or potential surfaces, which makes the model implementation into FE codes rather straightforward. Numerous applications of the hypoplastic models to boundary value problems document the possible range of their employment and several results confronted with observations reveal a good coincidence with measured data [12, 28, 26, 11, 21].

The crucial point for the application of any model in the real world is the determination of model parameters (constants). The first generation of hypoplastic models was calibrated using selected points of element tests. Knowing all model (state) variables at those points, the model parameters could be obtained by solving the system of linear equations with the model parameters as unknowns [17]. However, such a procedure is quite sensitive to the selection of calibration points and it becomes very cumbersome for more complicated structure of model equations.

The requirement of the separability of model parameters, *i.e.* the possibility to determine the parameters independently of each other or at least in a sequence, was postulated by Gudehus [7] and first attempted by Bauer [1]. In the next step, a well-defined novel procedure for the determination of the hypoplastic parameters from properties of grain assemblies was established [9, 10]. This procedure yields a link to basic index characteristics of granular materials and thus closes the usual gap between a theoretical model formulation and its practical application outside the group of model developers.

The aim of this paper is to show limits of the granulometric approach in the determination of the hypoplastic parameters. After an overview of the standard procedure for determination of the parameters, which is well suited for sands, two extreme cases of granular soils will be discussed: a coarse-grained rockfill and a fine-grained loess. The discussion will be based on experimental results and different ways for obtaining the model parameters will be proposed. Finally, difficulties of applying the hypoplastic model for clays will be demonstrated.

2. Standard procedure for determination of model parameters

2.1 Hypoplastic equation

Throughout this paper the hypoplastic equation published by von Wolffersdorff [27] will be considered although the results presented here generally apply for other hypoplastic models as well. For the determination of parameters of the hypoplastic model it is sufficient to consider a compression of a cylindrical sample with $T_1 < T_2 = T_3$ ($T_{ij} = 0$ for $i \neq j$, compressive stresses and strains are negative). In this case fixed directions of the principal stresses T_j coincide with the principal stretchings D_j and the general hypoplastic equation is simplified to:

$$\dot{T}_i = \frac{f_s}{\hat{T}_1^2 + 2\hat{T}_2^2} \left[D_i + a^2 (\hat{T}_1 D_1 + 2\hat{T}_2 D_2) \hat{T}_i + f_d \frac{a}{3} (6\hat{T}_i - 1) \sqrt{D_1^2 + 2D_2^2} \right] \quad (1)$$

with $j = 1, 2$ and $\hat{T} = T_j / (T_1 + 2T_2)$. Using notions of the pressure-dependent relative density:

$$D_p = \frac{e_c - e}{e_c - e_d}, \quad (2)$$

and of the mean pressure:

$$p_s = -(T_1 + 2T_2)/3, \quad (3)$$

the scalar multipliers f_s and f_d in Equation (1) are defined as:

$$f_d = (1 - D_p)^\alpha, \quad (4)$$

$$f_s = \frac{1 + e_i}{e_i} \left(\frac{e_i}{e} \right)^\beta \frac{h_s}{n} \left(\frac{3p_s}{h_s} \right)^{1-n} \left[3 + a^2 - a\sqrt{3} \left(\frac{e_{i0} - e_{d0}}{e_{c0} - e_{d0}} \right)^\alpha \right]^{-1}, \quad (5)$$

with:

$$\frac{e_i}{e_{i0}} = \frac{e_c}{e_{c0}} = \frac{e_d}{e_{d0}} = \exp \left[- \left(\frac{3p_s}{h_s} \right)^n \right]. \quad (6)$$

There are altogether 8 material parameters in the hypoplastic equation: a , h_s , n , e_{i0} , e_{c0} , e_{d0} , α and β .

2.2 Critical state parameters

Consider Equation (1) in case of a large monotonic shear deformation. Due to the asymptotic properties of the hypoplastic model a critical state with:

$$\dot{T}_j = 0, \quad D_1 + 2D_2 = 0 \quad (D_1 \neq 0) \quad \text{and} \quad e = e_c$$

will be approached. For a standard triaxial compression test in which a cylindrical sample is compressed axially at a constant lateral stress ($\dot{T}_2 = 0$), and using $\dot{T}_1 + 2\dot{T}_2 = 0$, Equation (1) reduces to:

$$a(T_1 - T_2) - \sqrt{\frac{3}{2}}(T_1 + 2T_2) = 0. \quad (7)$$

Inserting the definition of the critical friction angle:

$$\sin \varphi_c = \left(\frac{T_1 - T_2}{T_1 + T_2} \right)_c$$

one obtains a relation between a and φ_c :

$$a = \frac{\sqrt{3}(3 - \sin \varphi_c)}{2\sqrt{2} \sin \varphi_c}. \quad (8)$$

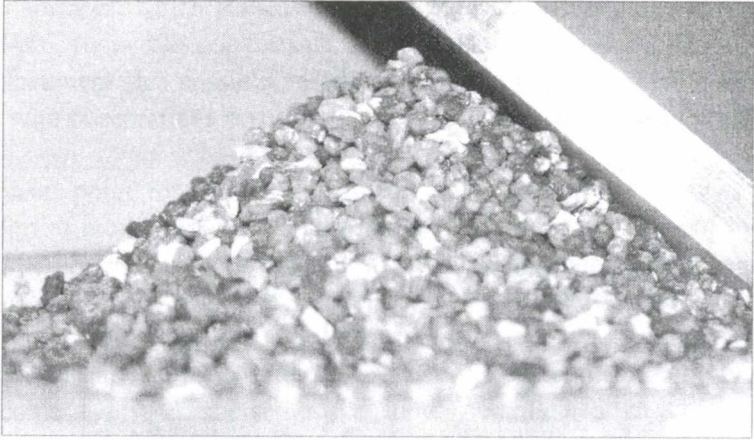


Figure 1. Measuring the angle of repose

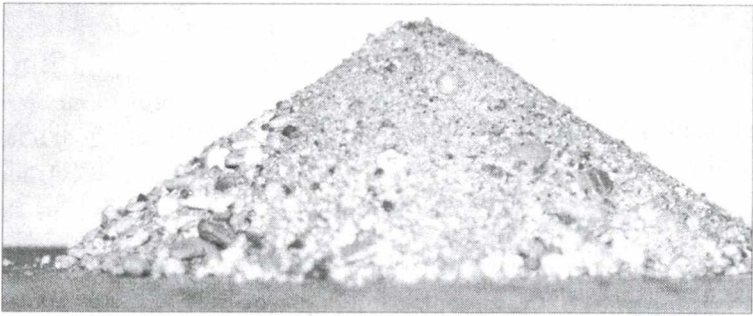


Figure 2. Grain size segregation of a gravelly sand

φ_c can be estimated from the angle of repose if cohesive forces are negligible (Figure 1). φ_c depends mainly on the grain size and angularity, being only a little affected by nonuniformity of the grain size distribution [10]. For well-graded granular soils a segregation of grain sizes may be observed during the construction of the soil heap (Figure 2). However, this effect does not seem to influence the angle of repose significantly.

The critical void ratio e_{c0} is the second parameter related to the critical state. It is defined at zero pressure, hence no direct measurement is possible. Nevertheless, a change of e_c with p_s has been the topic of many experimental studies enabling an extrapolation of $e_c - p_s$ - curves to $p_s = 0$. It can be observed [23, 10] that $e_{c0} = e_{max}$. This can be explained by reaching a critical state in standard index experiments for the determination of e_{max} in which granular materials undergo large shear deformations at very low pressures. e_{max} shows a good correlation with the granulometric properties [14, 31] as it decreases with increasing nonuniformity of the grain size distribution and decreasing angularity of grains.

2.3 Limit void ratios

The parameter e_{i0} denotes the maximum void ratio at zero pressure which can be theoretically reached during isotropic consolidation of grain suspension in a gravity-free space. During further isotropic compression e_i is assumed to decrease with increasing mean pressure after Equation (6). The standard index value of e_{max} must be lower than e_{i0} because of stress conditions during the e_{max} -experiment.

Let us consider the case of a skeleton composed from identical spheres where the value of e_{i0} corresponds to the theoretical maximum void ratio of a regular array of spheres, *i.e.* $e_{i0} = 0.91$. Comparing this value with the experimentally measured $e_{max} \approx 0.75$ for glass spheres [9], the ratio $e_{i0}/e_{max} \approx 1.20$ is obtained which can be used for estimation of e_{i0} from e_{max} . For well-graded granular materials it can be assumed that the ratio e_{i0}/e_{max} is slightly lower, *e.g.* $e_{i0}/e_{max} = 1.15$.

In analogy to e_i the pressure-dependent minimum void ratio e_d also bounds the allowable states of soil. It is supposed that the maximum density, which can be reached only by means of cyclic shearing with small amplitude under constant pressure, increases with p_s according to Equation (6) similarly to e_i . The value of e_d at zero pressure, e_{d0} , is very close to the index value of e_{min} . This results from limited densification using standard methods for the determination of e_{min} ; the soil density does not reach e_d which is compensated by assuming a zero pressure although during the test a non-zero pressure level exists.

2.4 Parameters describing proportional compression

The decrease of e_i with increase of p_s is modelled by Equation (6) using the constants h_s and n . This relation describes a stress-strain curve for any proportional compression (*i.e.* compression with constant ratio of components D_j) which starts from the void ratio e_{p0} at pressure zero:

$$e_p = e_{p0} \exp \left[- \left(\frac{3p_s}{h_s} \right)^n \right]. \quad (9)$$

It should be emphasized that e_p can correspond to e_i in case of isotropic compression but it may not become e_c or e_d ! Two latter variables characterize asymptotic states of the soil behaviour and they are not related to any stress-strain curve. The value e_{p0} is bounded by $e_{i0} \geq e_{p0} \geq e_{c0}$ and it is uniquely determined by the particular direction of stretching [1]. Consequently, for the experimental determination of h_s and n , a relatively demanding isotropic compression test can be replaced by a simpler oedometer test. Small variations of the experimental initial void ratio do not influence the shape of the measured curve [9]. It is thus sufficient to prepare the specimen at a void ratio close to e_{max} .

The exponent n mainly reflects the curvature of the compression curve and it can be calculated as:

$$n = \frac{\ln\left(\frac{e_1 \lambda_2}{e_2 \lambda_1}\right)}{\ln\left(\frac{p_{s2}}{p_{s1}}\right)}, \tag{10}$$

see Figure 3, with the compression index λ defined as $\lambda = \Delta e / \Delta \ln(p_s / p_{s0})$. Convincing correlations with the nonuniformity coefficient of the grain size distribution and the mean grain size were found for various sands [9, 10]. The parameter h_s is called *granulate hardness* [7], has a dimension of stress and can be obtained with the already calculated n from:

$$h_s = 3 p_s \left(\frac{ne}{\lambda}\right)^{1/n} \tag{11}$$

for any λ within the pressure range $p_{s1} \leq p_s \leq p_{s2}$ with the corresponding e .

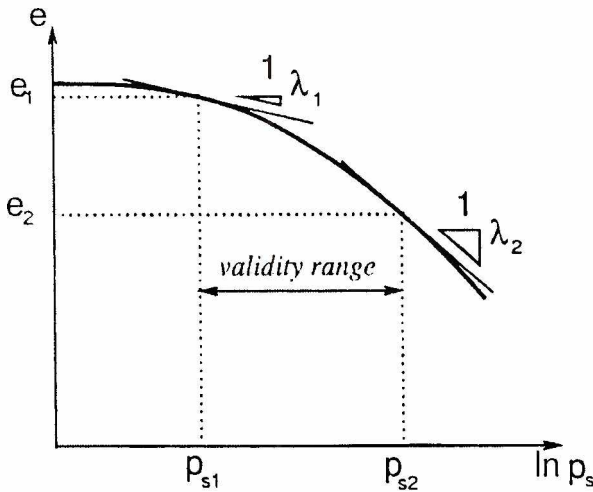


Figure 3. Determination of the exponent n

2.5 Exponents α and β

During shearing of an initially dense grain skeleton at constant mean (or lateral) pressure, a peak value of the friction angle $\varphi_p > \varphi_c$ can be observed. The difference between φ_c and φ_p increases with the increase of the pressure-dependent relative density and its value is controlled by the exponent α , see Equation (4). Knowing the axial stress T_1 and the void ratio e at peak of the stress-strain curve (*i.e.* when $\dot{T}_1 = 0$) in a standard triaxial test with constant lateral stress $\dot{T}_2 = 0$, the value of α can be calculated from Equation (1). Figure 4 shows the results of such calculations for $D_p = 0.8$.

The exponent β , see Equation (5), is the last parameter of the hypoplastic model to be determined. With:

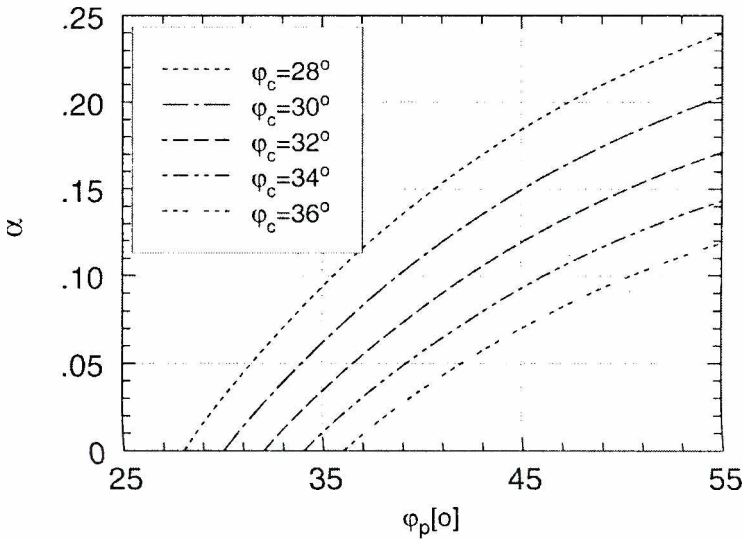


Figure 4. Relation between α , φ_p and φ_c for $D_p = 0.8$

$$\beta_0 = \frac{3 + a^2 - a\sqrt{3}f_{d1}}{3 + a^2 - a\sqrt{3}f_{d2}} \quad (12)$$

one can calculate β from the ratio of incremental stiffness moduli, $E = \dot{T}_1/D_1$, at the same mean pressures but at two different void ratios $e_1 = e_{loose}$ and $e_2 = e_{dense}$ during isotropic compression:

$$\beta = \frac{\ln\left(\beta_0 \frac{E_2}{E_1}\right)}{\ln\left(\frac{e_1}{e_2}\right)} \quad (13)$$

A similar equation for β can be written also for the case of oedometric compression [9]. For a particular mean pressure E usually increases proportionally with decreasing e , and $\beta \approx 1$ is valid for many sands [10].

3. Coarse-grained soils

The behaviour of coarse-grained soils does not differ too much from the behaviour of sands. However, additional difficulties arise during laboratory experiments because soils with large grains cannot be usually tested in common experimental devices. One has often to improvise and make use of available equipment.

A limestone rockfill, which was used for the determination of the hypoplastic parameters, has the specific weight $\rho_s = 2.72 \text{ g/cm}^3$ and was obtained by rock crushing. This resulted in angular grains and a very broad grain size distribution with the nonuniformity coefficient $C_u \approx 20$ (10% of weight were grains larger than 60 mm, 7% were within the sand fraction and the silty fraction was below 3%). The

angle of repose was measured in a traditional way, although using a motor jack and a special funnel, see Figure 5. From a soil heap, which was 40 cm high, the angle of repose $\varphi_c = 38^\circ$ could be determined. Although the grain segregation was neglected, this value corresponds very well to the value of φ measured in triaxial tests on the loose dolomite railroad ballast [22]. It can be inferred that φ_c depends predominantly on the grain shape, and the influence of grain size and grain size distribution is only of minor importance. Similar values of φ_c were namely measured also in case of crushed sands with much smaller grains [13].

The maximum void ratio $e_{max} = 0.68$ was obtained by careful filling of the material with a shovel into a cylindrical container (diameter 510 mm). The parameter e_{i0} was calculated as $e_{i0} = 1.15 e_{max} = 0.782$. The minimum void ratio was measured after shaking the specimen in a cylinder with $D = 100$ mm. For this purpose only grains smaller than 16 mm were selected and $e_{min}^* = 0.43$ was measured. This value is certainly influenced by different grading. Therefore, using the latter container and the latter soil without larger grains the maximum void ratio $e_{max}^* = 0.94$ was determined. From the ratio $e_{max}^*/e_{min}^* = 2.18$ the value $e_{min} = e_{max}/2.18 = 0.31$ was calculated which is close to $e = 0.36$ measured by the Proctor test.

In order to determine the parameters h_s and n a compression test was performed using a special thick wall steel cylinder of 510 mm in diameter (Figure 6). The naturally dry specimen was prepared by shovelling and was compressed axially applying the pressure in steps by a hydraulic jack. The measured experimental curve is denoted as *loose* in Figure 7. From $\lambda = 0.037$ at $T_1 = -30$ kPa ($e = 0.662$) and $\lambda = 0.084$ at $T_1 = -700$ kPa ($e = 0.472$), assuming $T_2/T_1 = 1 - \sin \varphi_c$ and using Equations (10) and (11), the following values could be determined: $h_s = 10$ MPa and $n = 0.36$.

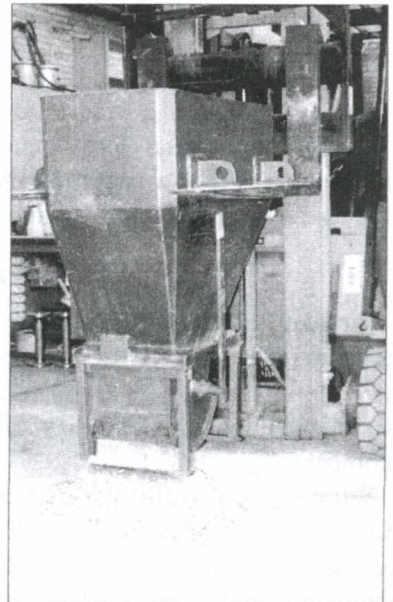
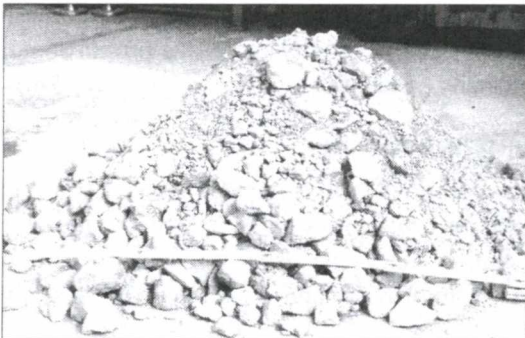


Figure 5. Measuring the angle of repose of limestone rockfill

No triaxial tests on the limestone rockfill were performed thus only an estimation of α is possible. The published results of triaxial compression tests on the dolomite railroad ballast [22] reveal $\varphi_p \approx 55^\circ$ for a dense packing at low cell pressures. Using this value, $\varphi = 38^\circ$ and Figure 4, the parameter $\alpha = 0.10$ can be found.

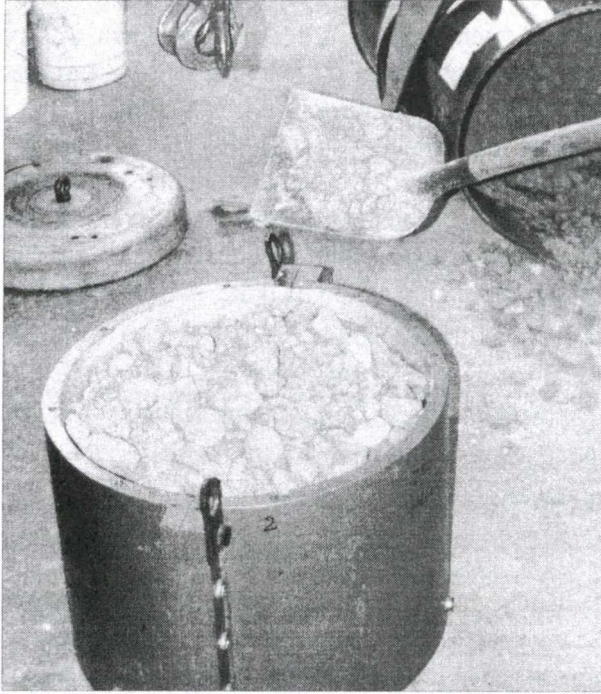


Figure 6. Specimen preparation for oedometer test

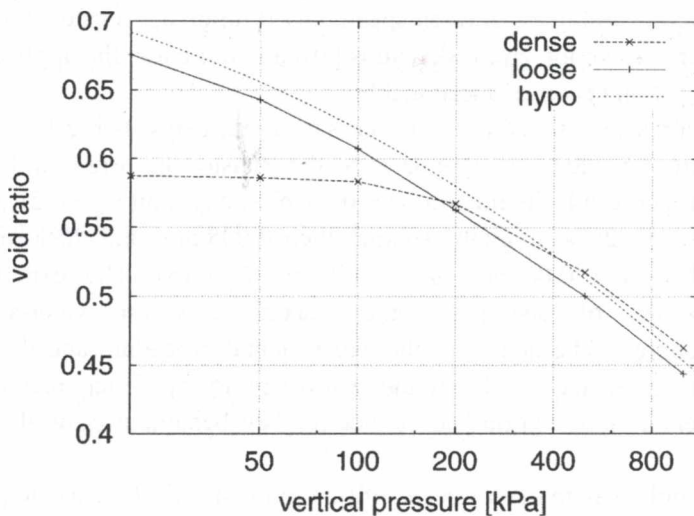


Figure 7. Measured oedometer curves of the limestone rockfill (dense, loose) and the hypoplastic equation (hypo)

Table 1. Parameters of the hypoplastic model for limestone rockfill

φ [°]	\hat{h}_s [MPa]	n	e_{d0}	e_{c0}	e_{r0}	α	β
38.0	10.0	0.36	0.31	0.68	0.78	0.10	3.1

One additional oedometer test with a dense specimen was performed, which was intended for the determination of β . A higher density was reached by tamping of soil layers while filling the oedometer cell. Nevertheless, the initial void ratio $e = 0.59$ was far above the value $e_{min} = 0.31$ and the measured curve (Figure 7, denoted as *dense*) reached the curve of an initially loose specimen at higher pressures. The tamping was obviously not heavy enough for a sufficient densification of the soil. Hence, a direct application of Equation (13) was not possible and, similarly like for α , an estimation had to be done. A comparison of stiffness moduli at lower pressures ($T_1 > -100$ kPa) yields $E_{dense}/E_{loose} \geq 10$. Considering $a = 0.79$ for $\varphi_c = 38^\circ$ and extreme values $f_{d1} = 1$ and $f_{d2} = 0$, the value $\beta_0 = 0.8$ is obtained (for other values of f_{di} approaches $\beta_0 \rightarrow 1$). Assuming realistic void ratios $e_1 = 0.65$ and $e_2 = 0.33$ and using $E_2/E_1 = 10$, Equation (13) now yields $\beta = 3.07$. A summary of the hypoplastic parameters of the limestone rockfill is in Table 1.

4. Fine-grained soils

Fine-grained soils introduce other difficulties for the application of the hypoplastic model. Contrary to the coarse-grained soils there are no problems with the specimen size. However, physico-chemical interaction forces between the grains disable an employment of the outlined standard procedure for the determination of material parameters. It is clear that the angle of repose or experiments for measuring e_{max} and e_{min} become meaningless. Moreover, with decreasing grain size a single grain is more difficult to define and one can often speak only of grain aggregates. Such soils cannot be considered as simple grain skeletons [10] any more and the application of the hypoplastic equation becomes questionable.

Loess soils represent a transition between sands and clays, being typical silty soils. The loess from Sedlec near Prague is of the Pleistocene origin and has the following index properties [4]: liquid limit $w_l = 0.36$, plasticity limit $w_p = 0.21$, specific weight $\rho_s = 2.7$ g/cm³, 20% of grains smaller than 0.005 mm and 70% of grains in the range 0.005 and 0.06 mm ($d_{50} \approx 0.02$ mm, $C_u \approx 15$). The experimental programme consisted of oedometer and triaxial tests on water-saturated reconstituted specimens. The details of the experimental procedure and discussion of the experimental results can be found elsewhere [5, 6]. Since reconstituted specimens represent a loose “virgin” soil structure, their behaviour is similar to that of a loose sand.

There is no simple way to determine φ_c of fine-grained soils. One has to perform shear tests, either in a direct shear box or in a triaxial cell. The first type of the test is simpler but it is not an element test and thus the evaluation of test results may be

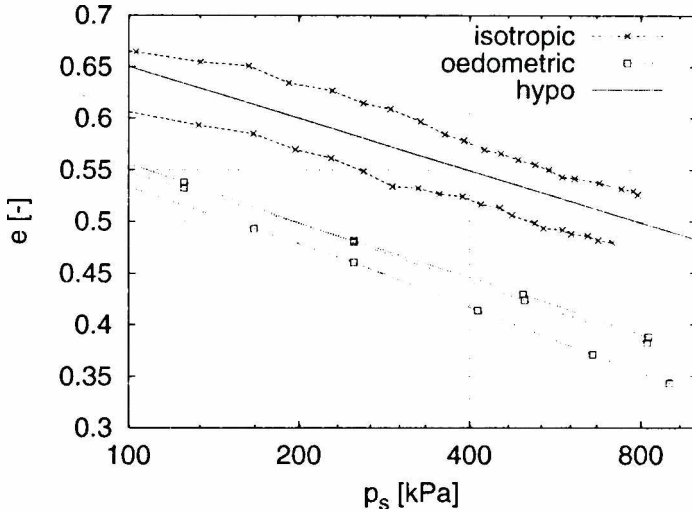


Figure 8. Comparison of experimental compression curves of loess (isotropic, oedometric) with the calculated curve (hypo)

problematic. A triaxial test, if provided with frictionless specimen ends, can be treated as a real element test at least up to the peak. The peak states in triaxial tests on the reconstituted loess yielded $\varphi_c = 30^\circ$ which is the value that many sands have. This fact is not so surprising: the loess grains are rather similar to downscaled sand grains [19].

Compression tests were performed not only as one-dimensional compression in the oedometer ring but also as isotropic compression in the triaxial cell. Reconstituted specimens ensure that the compression tests can be treated as proportional compressions. The measured curves from both test types, see Figure 8 ($K_0 = 1 - \sin \varphi_c = 0.5$ was considered for the evaluation of oedometer tests), reveal an almost linear e vs. $\log p_s$ relationship with $\lambda = 0.073$. This logarithmic relation is equivalent with:

$$\dot{p}_s = \frac{p_s}{\lambda} \dot{e}. \tag{14}$$

Rewriting Equation (9) into the rate form yields [9]:

$$\dot{p}_s = \xi \left(\frac{3p_s}{h_s} \right)^{1-n} \frac{\dot{e}}{e}, \tag{15}$$

where $e = e_p$ and $\xi = const.$ It seems that choosing $n = 0$ one obtains a similar relation like Equation (14). Unfortunately, the constant ξ reads:

$$\xi = -\frac{h_s}{3n} \tag{16}$$

and hence $n = 0$ is not allowed.

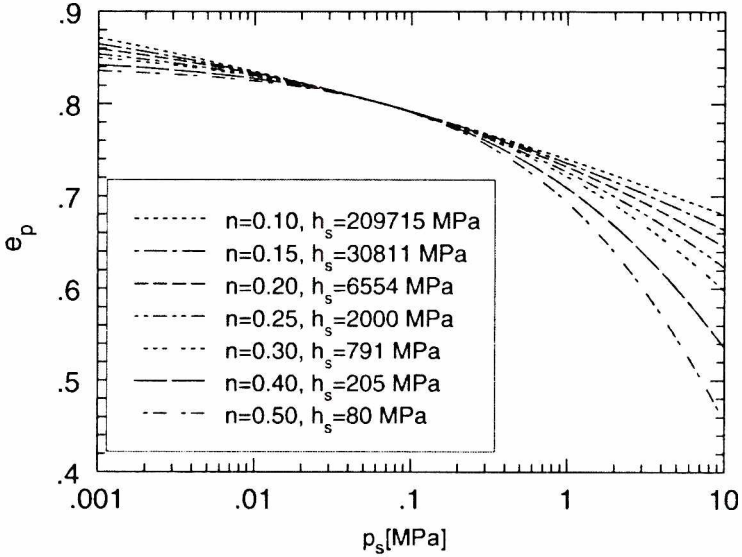


Figure 9. All calculated compression curves yield the same $\lambda = 0.020$ at $p_s = 0.1$ MPa

Figure 9 shows numerical representations of Equation (9) for different values of h_s and n . The choice of the parameters was done in such a way to get always the same λ at one particular pressure. It can be noticed that, in spite of very different overall performance, all calculated curves fall almost together for p_s between 0.01 and 0.3 MPa and they look rather linear in this pressure range.

Inserting $\lambda_1 = \lambda_2$ into Equation (10) enables immediately a calculation of n . Returning to the experiments with loess, taking $e_1 = 0.65$ at $p_{s1} = 100$ kPa and $e_2 = 0.5$ at $p_{s2} = 800$ kPa results in $n = 0.126$. The granulate hardness $h_s = 0.79$ MPa then follows from Equation (11) for $\lambda = 0.073$, $p_s = 0.2$ MPa and $e = 0.6$.

The determination of e_{max} and e_{min} must be replaced by another kind of test. It can be considered that the isotropic compression of the reconstituted sample is close to the e_i -curve. Knowing h_s and n the value of e_{i0} can be back-calculated from:

$$e_{i0} = e_i \exp \left[\left(\frac{3p_s}{h_s} \right)^n \right]. \tag{17}$$

For $e = e_i = 0.60$ at $p_s = 0.2$ MPa, $e_{i0} = 1.58$ and $e_{c0} = e_{i0} / 1.15 = 1.37$ follow.

It was already recognized by Casagrande that the liquid limit test is analogous to a shear test [25]. Thus in case of water saturated soil w_l is related to $e_c = w_l \rho_s / \rho_w$ (ρ_s and ρ_w are the specific weights of soil and water). Estimating the maximal mean pressure $p_l \approx 5$ kPa during each blow [7], e_{c0}^* can be calculated as:

$$e_{c0}^* \approx w_l \frac{\rho_s}{\rho_w} \exp \left[\left(\frac{3p_l}{h_s} \right)^n \right]. \tag{18}$$

For $w_i = 0.36$ one gets $e_{c0}^* = 1.78$ which is substantially higher than the previously calculated value of 1.37. There may be two reasons for the difference. First, the initial state of the reconstituted specimen did not lie on the e_i -curve because the soil was already densified during remoulding. Second, the value of p_i is overestimated (however, a good coincidence would be reached for $p_i = 0.1$ kPa which seems to be too low). In reality there is probably an interplay of both factors.

Concerning e_{min} , Gudehus [7] proposed that the cracking of the soil specimen during the plastic limit test is due to the soil dilatancy when the maximum densification in cyclic shearing is reached (at the associated mean pressure $p_p \approx 15$ kPa). Therefore:

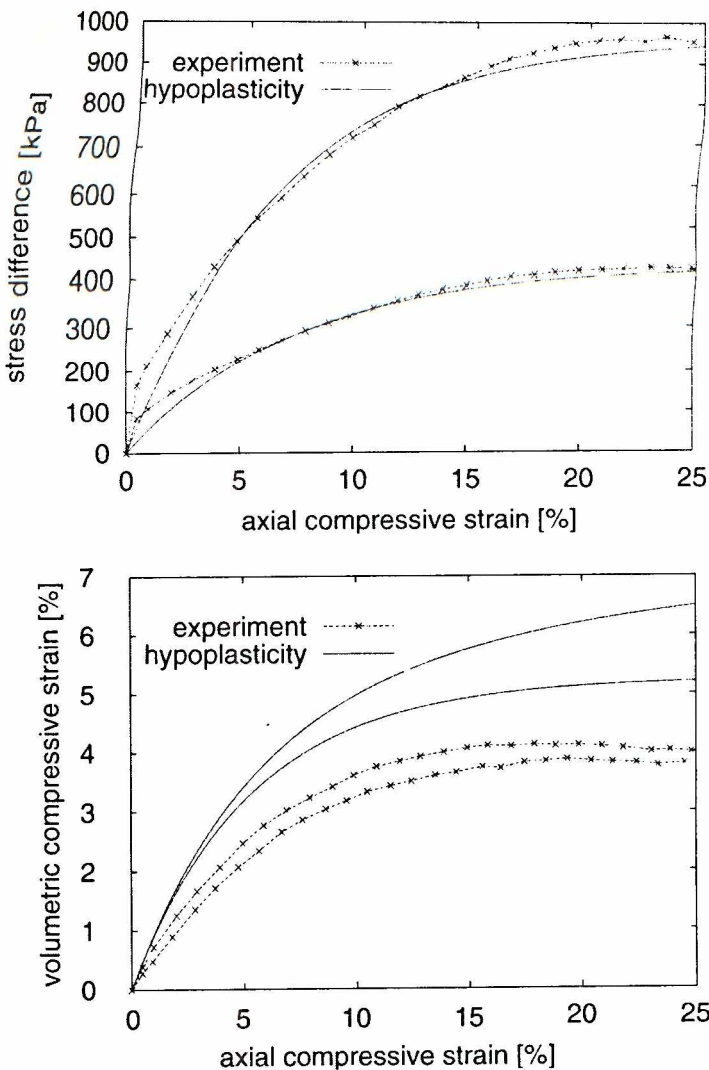


Figure 10. Recalculation of triaxial tests with Sedlec loess for the cell pressures 200 and 500 kPa

$$e_{d0}^* \approx w_p \frac{\rho_s}{\rho_w} \exp \left[\left(\frac{3p_p}{h_s} \right)^n \right]. \quad (19)$$

Using $h_s = 0.79$ MPa and $n = 0.126$ one gets $e_{d0}^* = 1.14$. If the difference $e_{c0}^* - e_{d0}^* = 1.78 - 1.14 = 0.64$ is taken as a soil characteristic, one can obtain $e_{d0} = 0.73$ corresponding to $e_{c0}^* = 1.37$.

There are no triaxial and oedometer experiments available for the case of dense loess specimens. Consequently, α and β can only be estimated analogously to the parameters of gravel. In a first approximation the values typical for sands, e.g. $\alpha = 0.15$ and $\beta = 1.0$ [10], can be used.

Table 2. Parameters of the hypoplastic model for Sedlec loess

φ [°]	h_s [MPa]	n	e_{d0}	e_{c0}	e_{d0}^*	α	β
30	0.79	0.126	0.73	1.37	1.58	0.15	1.0

The hypoplastic parameters of Sedlec loess from Table 2 were applied for the recalculation of triaxial tests, see Figure 10. It can be noticed that there is a good agreement between the experiment and the theory, especially in case of the stress-strain curves. The volumetric strains calculated by the hypoplastic model seem to be overpredicted. It must be pointed out, however, that the calculated volumetric strains depend significantly on the initial void ratio. There may be minor error in the experimentally determined values $e = 0.57$ for $T_2 = -200$ kPa and $e = 0.55$ for $T_2 = -500$ kPa which can influence the depicted comparison.

5. Clays

The preceding section could imply that the hypoplastic model is also suitable for the description of the behaviour of clays. The outlined procedure for the determination of the hypoplastic parameters of loess can be namely applied for clays as well. However, as it will be shown in the sequel, the hypoplastic model without modification is not suitable for the description of clays.

It is widely accepted that the behaviour of soft (normally consolidated) clayey soils under axisymmetric conditions can be well described by the Modified Cam Clay constitutive model. For the initially isotropic stress state and assuming the plastic deformation, the axial strain rate according to the Modified Cam Clay Model is given by [29]:

$$\dot{\varepsilon}_a = \frac{\lambda}{9(1+e)p_s} (\dot{\sigma}_a + 2\dot{\sigma}_r) + \frac{1}{3G} (\dot{\sigma}_a - \dot{\sigma}_r). \quad (20)$$

G denotes the elastic shear modulus, and σ_a and σ_r are the axial and radial effective stresses (λ is a compression index during the virgin compression). Contrary to the hypoplasticity the Cam Clay model is formulated within the small-strain theory and it

uses the geotechnical convention of positive compressive stresses and strains. From Equation (20) it can be immediately seen that the stiffness in the isotropic stress state is *independent* of any limit stress state parameter (like φ_c). The stiffness at the beginning of the triaxial compression ($\dot{\sigma}_r = 0$) corresponds to:

$$E_{tr}^{cc} = \frac{\dot{\sigma}_a}{\dot{\epsilon}_a} = \frac{3}{\frac{\lambda}{3(1+e)p_s} + \frac{1}{G}}, \quad (21)$$

and

$$E_{iso}^{cc} = \frac{\dot{\sigma}_a}{\dot{\epsilon}_a} = \frac{3(1+e)p_s}{\lambda} \quad (22)$$

is the stiffness during the isotropic compression ($\dot{\sigma}_a = \dot{\sigma}_r$). The ratio of both stiffnesses is equal to:

$$\frac{E_{iso}^{cc}}{E_{tr}^{cc}} = \frac{1}{3} + \frac{p_s(1+e)}{\lambda G}. \quad (23)$$

Because λ is related to the bulk modulus $K = \dot{p}_s / \dot{\epsilon}_v$ via:

$$\lambda = \frac{p_s(1+e)}{K} \quad (24)$$

and

$$K = \frac{2G(1+\nu)}{3(1-2\nu)}, \quad (25)$$

the ratio of the stiffness moduli can be written as

$$\frac{E_{iso}^{cc}}{E_{tr}^{cc}} = \frac{1}{3} + \frac{K}{G} = \frac{1}{3} + \frac{2(1+\nu)}{3(1-2\nu)}, \quad (26)$$

which is a function of Poisson ratio ν only! From the graphical representation of Equation (26) in Figure 11 it can be seen that for realistic values $0 \leq \nu \leq 0.35$ the stiffness ratio E_{iso}^{cc}/E_{tr}^{cc} is smaller than 3.

Let us now perform the same comparison for the hypoplastic model. The hypoplastic equation for the isotropic compression reads:

$$\dot{T}_1 = f_s (3 + a^2 - f_d a \sqrt{3}) D_1. \quad (27)$$

In case of the standard triaxial compression ($\dot{T}_2 = 0$) one has a set of two equations:

$$\dot{T}_1 = 3f_s \left[D_1 + \frac{a^2}{9} (D_1 + 2D_2) + f_d \frac{a}{3} \sqrt{D_1^2 + 2D_2^2} \right], \quad (28)$$

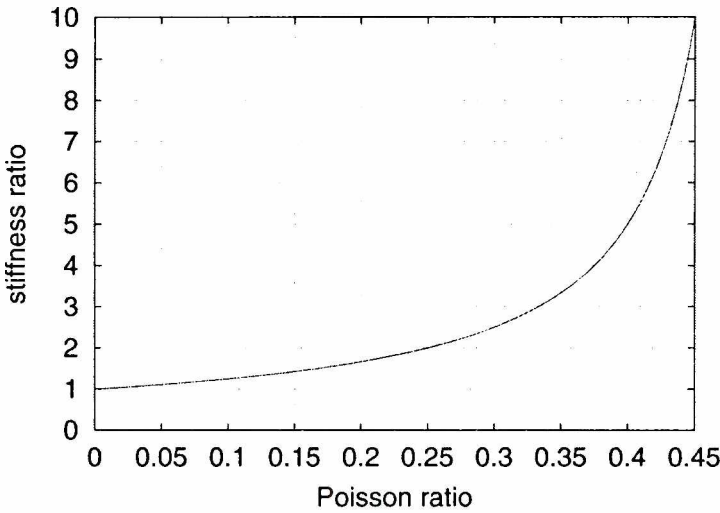


Figure 11. Relation between E_{iso}^{cc}/E_{ix}^{cc} and ν for the Modified Cam Clay Model

$$0 = D_2 + \frac{a^2}{9}(D_1 + 2D_2) + f_d \frac{a}{3} \sqrt{D_1^2 + 2D_2^2}. \quad (29)$$

In both equations the multiplier f_d is state-dependent. Without loss of generality one can consider the density in the critical state of soil, $f_d = 1$, since the stiffnesses can be compared for an arbitrary (allowed) state. Thus one can write:

$$E_{iso}^{hyp} = f_s (3 + a^2 - a\sqrt{3}), \quad (30)$$

$$E_{ix}^{hyp} = 3f_s (1 + D_2/D_1) = 3f_s (1 - \nu_{ix}), \quad (31)$$

and consequently:

$$\frac{E_{iso}^{hyp}}{E_{ix}^{hyp}} = \frac{3 + a^2 - a\sqrt{3}}{3(1 - \nu_{ix})}. \quad (32)$$

Although the parameter ν_{ix} is not free (it follows from the solution of the system of Equations (28) and (29) and the condition of rate independence $\sqrt{D_1^2 + 2D_2^2} = 1$ for a given set of material parameters), its value is usually within the range $0 \leq \nu_{ix} \leq 0.3$. However, the further parameter a , which is a function of the critical friction angle φ_c , can vary significantly. From the plotted dependence between φ_c and $E_{iso}^{hyp}/E_{ix}^{hyp}$ in Figure 12 it is obvious that for $\varphi_c < 25^\circ$ the stiffness ratio becomes too high. For $\nu_{ix} > 0$ this problem is encountered even at higher φ_c . Consequently, the hypoplastic Equation (1) cannot be applied for a realistic modelling of soils with low φ_c , *i.e.* especially for clays.

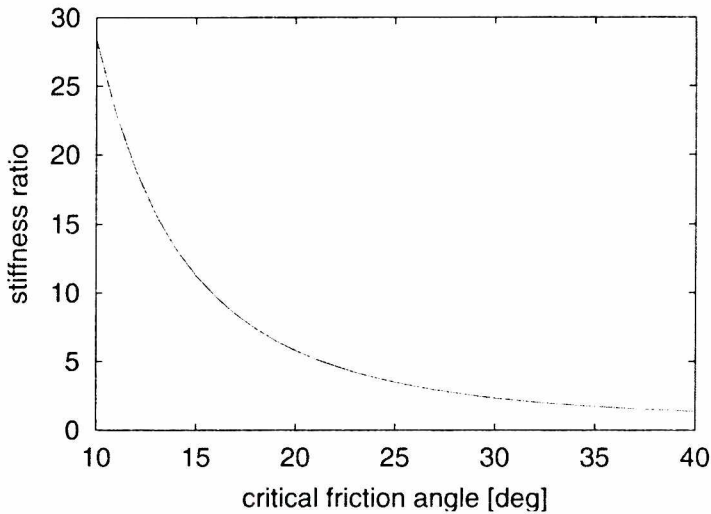


Figure 12. Relation between $E_{iso}^{hyp}/E_{tc}^{hyp}$ and ϕ_c for the hypoplastic model ($\nu_n = 0$)

6. Conclusions

The hypoplastic model is well-suited for the mathematical description of the mechanical behaviour of granular materials. The simple procedure for the determination of the model parameters has already been successfully tested for various sands. However, there are limits to the application of this procedure. They result from a wide spectrum of granulometric properties of soils. In case of coarse-grained soils the application of the calibration procedure is mainly restricted by the available laboratory equipment. On the contrary, in case of fine-grained soils severe modifications of the calibration procedure must be undertaken. Nevertheless, for silty soils with rather high critical friction angles the hypoplastic parameters can be found and verified.

There is a significant problem for the application of the hypoplastic model (1) for clays which usually have low critical friction angles. In this case the basic structure of the hypoplastic equation yields an unrealistic ratio of incremental stiffnesses in isotropic and triaxial compression. Consequently, the model parameters cannot be properly determined.

Acknowledgement

The financial support by the Grant Agency of the Academy of Sciences of the Czech Republic (Grant No. B2071901) is gratefully acknowledged. Experiments on the limestone rockfill were performed during the author's stay at the Institute of Soil Mechanics and Rock Mechanics, University of Karlsruhe.

References

- [1] Bauer J., *Calibration of a comprehensive hypoplastic model for granular materials*, Soils and Foundations **36**, 13, 1996
- [2] Bauer E. and Herle I., *Stationary states in hypoplasticity*, in D. Kolymbas (editor), *Constitutive Modelling of Granular Materials*, 167, Horton, Springer, 2000
- [3] Chambon R., Desrues J., Hammad W. and Charlier R., *CLOE, a new rate-type constitutive model for geomaterials*, Theoretical basis and implementation, *International Journal for Numerical and Analytical Methods in Geomechanics* **18**, 253, 1994
- [4] Fedá J., *Collapse of loess upon wetting*, *Engineering Geology* **25**, 263, 1988
- [5] Fedá J., Boháč J. and Herle I., *Compression of collapsed loess: Studies on bonded and unbonded soils*, *Engineering Geology* **34**, 95, 1993
- [6] Fedá J., Boháč J. and Herle I., *End restraint in triaxial testing of soils*, *Acta Technica CSAV* **38**, 197, 1993
- [7] Gudehus G., *A comprehensive constitutive equation for granular materials*, *Soils and Foundations* **36**, 1, 1996
- [8] Gudehus G., *Attractors, percolation thresholds and phase limits of granular soils*, In Behringer and Jenkins (eds), *Powders and Grains*, 169, Balkema, 1997
- [9] Herle I., *Hypoplastizität und Granulometrie einfacher Korngerüste*, Veröffentlichungen des Institutes für Bodenmechanik und Felsmechanik der Universität Fridericiana in Karlsruhe, Heft 142, 1997
- [10] Herle I. and Gudehus G., *Determination of parameters of a hypoplastic constitutive model from properties of grain assemblies*, *Mechanics of Cohesive-Frictional Materials* **4**, 461, 1999
- [11] Herle I. and Mayer P. M., *Verformungsberechnung einer Unterwasserbetonbaugrube auf der Grundlage hypoplastisch ermittelter Parameter des Berliner Sandes*, *Bautechnik* **76**, 34, 1999
- [12] Hügel H.M., *Prognose von Bodenverformungen*, Veröffentlichungen des Institutes für Bodenmechanik und Felsmechanik der Universität Fridericiana in Karlsruhe, Heft 136, 1995
- [13] Koerner R.M., *Effect of particle characteristics on soil strength*, *Journal of the Soil Mechanics and Foundations Division ASCE* **96**, 1221, 1970
- [14] Kolbuszewski J. and Frederick M., *The significance of particle shape and size on the mechanical behaviour of granular materials*, In Proc. ECSMF, Wiesbaden, 253, 1963
- [15] Kolymbas D., *A generalized hypoelastic constitutive law*, In Proc. XI Int. Conf. Soil Mechanics and Foundation Engineering, **5**, 2626, San Francisco, Balkema, 1985
- [16] Kolymbas D., *An outline of hypoplasticity*, *Archive of Applied Mechanics*, **61**, 143, 1991
- [17] Kolymbas D. and Bauer E., *Soft oedometer — a new testing device and its application for the calibration of hypoplastic constitutive laws*, *Geotechnical Testing Journal* **16**, 263, 1993
- [18] Kolymbas D., Herle I. and von Wolffersdorff P. A., *Hypoplastic constitutive equation with back stress*, *International Journal for Numerical and Analytical Methods in Geomechanics* **19**, 415, 1995

-
- [19] Mitchell J., *Fundamentals of soil behavior*, John Wiley & Sons, New York, second edition, 1993
- [20] Niemunis A. and Herle I., *Hypoplastic model for cohesionless soils with elastic strain range*, *Mechanics of Cohesive-Frictional Materials* **2**, 279, 1997
- [21] Nübel K. and Cudmani R., *Examples of finite element calculations with the hypoplastic law*, In: Kolymbas D. (ed.), *Constitutive Modelling of Granular Materials*, pages 523–538, Springer, 2000
- [22] Raymond G.P. and Davies J.R., *Triaxial tests on dolomite railroad ballast*, *Journal of Geotechnical Engineering ASCE* **104(GT6)**, 737, 1978
- [23] Riemer M.F., Seed R.B., Nicholson P.G. and Jong H. L., *Steady state testing of loose sands: limiting minimum density*, *Journal of Geotechnical Engineering ASCE* **116**, 332, 1990
- [24] Schofield A. and Wroth C., *Critical state soil mechanics*, McGraw-Hill, London, 1968
- [25] Seed H.B., Woodward R.J. and R.Lundgren, *Fundamental aspects of the Atterberg limits*, *Journal of the Soil Mechanics and Foundations Division ASCE* **90(SM6)**, 75, 1964
- [26] Tejchman J. and Herle I., *A "class A" prediction of the bearing capacity of plane strain footings on sand*, *Soils and Foundations* **39**, 47, 1999
- [27] von Wolffersdorff P. A., *A hypoplastic relation for granular materials with a predefined limit state surface*, *Mechanics of Cohesive-Frictional Materials* **1**, 251, 1996
- [28] von Wolffersdorff P. A., *Verformungsprognosen für Stützkonstruktionen*, Veröffentlichungen des Institutes für Bodenmechanik und Felsmechanik der Universität Fridericiana in Karlsruhe, Heft 141, 1997
- [29] Wood D.M., *Soil behaviour and critical state soil mechanics*, Cambridge University Press, Cambridge, 1990
- [30] Wu W., Bauer E. and Kolymbas D., *Hypoplastic constitutive model with critical state for granular materials*, *Mechanics of Materials* **23**, 45, 1996
- [31] Youd T., *Factors controlling maximum and minimum densities of sands*, In: *Evaluation of relative density and its role in geotechnical projects involving cohesionless soils*, STP 523, 98, ASTM, 1973